Using Superelement Model in Active Thermal Cycle with Temperature Dependent Properties

Junyan He, Henan Mao, and Adarsh Chaurasia
Synopsys, Inc
675 Almanor Ave
Sunnyvale, CA 94085 US
Email: hejimmy@synopsys.com

Abstract

Superelement (SE) is a modeling technique where the assembled stiffness matrix of a fully meshed model is reduced to a smaller subset of master degrees of freedom (DOFs) while condensing out internal DOFs with methods like Guyan reduction. The reduced stiffness matrix and its remaining master DOFs act as one SE in subsequent analysis to represent the stiffness behavior of the original meshed model. SE can be used to obfuscate critical intellectual property (IP) in the chip package design including internal geometry and part material properties, creating an obfuscated version of the chip that can be shared and used in board-level reliability simulations. However, traditional SE implementation based on Guyan reduction leads to a constant SE reduced stiffness matrix, therefore, it is not able to account for temperature-dependent material properties which have significant effects during thermal cycling. Previous research explored superimposing multiple SEs, each evaluated at a different (albeit uniform) temperature to capture temperature-dependent material properties in passive thermal cycling. This presentation expands on this concept and explores an extension to active thermal cycling where the temperature distribution within the chip package is not uniform. Using a generic example model, we demonstrated convergence to the full solid element behavior. A sensitivity study is performed to demonstrate robustness of the proposed method with respect to material property variations.

Key words

Superelement, Active thermal cycling, Temperature-dependent material properties

I. Introduction

Board-level electronics reliability analyses rely heavily on finite element simulations. To ensure analysis accuracy, different packages on the PCB need to be modeled accurately. However, the internal designs and material properties are often the core intellectual properties (IP) of chip manufacturers, making it impossible to share the detailed finite element model of the chip packages to suppliers for board-level analysis. Superelement (SE) [1,2] is a way to compactly represent the behavior of the chip package without revealing its internal structure and material properties. A SE model is a single finite element that serves as a condensed representation of a large group of regular solid finite elements. The SE model only exposes the necessary nodes (e.g., master nodes) to interact with the rest of the model assembly while hiding all internal nodes by condensing the assembled element stiffness matrix associated with the internal degrees of freedom. In summary, SE model only stores the information of a reduced stiffness matrix and does not reveal any details of the internal geometry of the chip package. Therefore, it allows protecting the core IP of the chip supplier. However, traditional SE formulations are limited to constant material properties, while material nonlinearity either due to temperature dependence or plasticity are present in realistic materials commonly used in electronics reliability analyses. Previous works in the literature [3] have investigated the different SE formulations to capture material nonlinearity due to plasticity. Nonlinearity due to temperature dependence has also been studied [4], where different SEs are generated at different prescribed constant temperatures to evaluate material properties at different temperatures, the resulting temperature-dependent SE is represented as a linear combination of the available SEs based on the known and constant temperature history. While this approach provides a pathway to capture temperature-dependence in SE, it is limited to constant temperatures (i.e., passive thermal cycling) and therefore not applicable to active thermal cycling where the chip package goes through a power cycle and leads to nonuniform temperature distribution within the chip and the PCB. In this work, we explore a workflow to generate temperature-dependent SE that accounts for the nonuniform temperature distribution during active thermal cycling. Examples are shown to demonstrate its usage in

active thermal cycling with comparison with the reference solution obtained by regular solid elements. A sensitivity study is conducted to demonstrate the robustness of the main assumption used in this proposed workflow.

II. Methods

A. Temperature-dependent SE generation (Generation pass)

Superelement is a condensed representation of the stiffness behavior of a structure in the form of a reduced stiffness matrix containing only selected master nodes. Different methods can be used to derive the reduced stiffness matrix, such as component mode synthesis [5] and Guyan reduction [6]. All examples in this work consider a Quad-Flat-No-leads (QFN) package and a PCB board, connected by solder. The solder and PCB are to be modeled as regular solid finite elements, and the entire QFN will be modeled by one SE. Active thermal cycling will be simulated where the QFN is cycled from 0 to 1W of applied power. The plastic work densities on the solder joints are the main quantities of interest to compare between the full solid element reference solution and the SE solution. Temperature-dependent material properties of copper, silicon die and mold compound are used within the QFN. Among them, the mold compound exhibits the strongest temperature-dependent nonlinearity with material properties taken from Fischer and Wilde [7] and is shown in Fig 1.

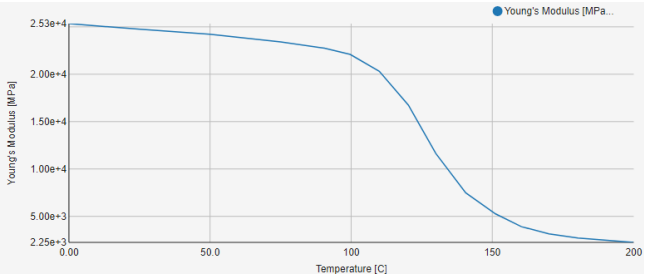


FIGURE 1: TEMPERATURE-DEPENDENT YOUNG'S MODULUS OF THE MOLD COMPOUND

Consider the finite element-discretized matrix equation for a finite element model:

$$\boldsymbol{K}\boldsymbol{u} = \boldsymbol{F} \tag{1}$$

where $\boldsymbol{K}$, $\boldsymbol{u}$, $\boldsymbol{F}$ denote the global FE stiffness matrix, nodal DoF, and load vector, accordingly. The DoFs can be partitioned into two groups, one involving DoFs on the interface of the SE and regular solid finite elements, and the other includes all other DoFs to be condensed out (denoted by subscript c):

$$\begin{bmatrix} \boldsymbol{K_{mm}} & \boldsymbol{K_{mc}} \\ \boldsymbol{K_{cm}} & \boldsymbol{K_{cc}} \end{bmatrix} \begin{bmatrix} \boldsymbol{u_m} \\ \boldsymbol{u_c} \end{bmatrix} = \begin{bmatrix} \boldsymbol{F_m} \\ \boldsymbol{F_c} \end{bmatrix} \tag{2}$$

Since interaction with other regular finite elements only occur on the master DoFs, only those DoFs are retained on the SE and all other DoFs are condensed by expressing them in terms of the master DoFs:

$$\boldsymbol{u_c} = \boldsymbol{K_{cc}^{-1}}(\boldsymbol{F_c} - \boldsymbol{K_{cm}}\boldsymbol{u_m}) \tag{3}$$

Substituting (3) into (2) and retaining only the master DoFs, one gets:

$$(\boldsymbol{K_{mm}} - \boldsymbol{K_{mc}}\boldsymbol{K_{cc}^{-1}}\boldsymbol{K_{cm}})\boldsymbol{u_m} = (\boldsymbol{F_m} - \boldsymbol{K_{mc}}\boldsymbol{K_{cc}^{-1}}\boldsymbol{F_c}) \tag{4}$$

This process generates the constant reduced stiffness matrix $\boldsymbol{K_r} = (\boldsymbol{K_{mm}} - \boldsymbol{K_{mc}}\boldsymbol{K_{cc}^{-1}}\boldsymbol{K_{cm}})$ of the SE at the temperature where the full global stiffness matrix is being evaluated at. For electronics reliability analysis, a sequential thermal-stress analysis will be carried out. Therefore, SE generation will be repeated for thermal and structural analyses (first obtaining the thermal SE stiffness matrix then the structural stiffness matrix).

Similar to multilinear plasticity models, nonlinear temperature dependence of materials can be approximated by a piece-wise linear curve. This approximation, applied to the context of SE reduced stiffness matrix, can be expressed as (using a simple 2-point example):

$$\boldsymbol{K_{r,@50^{\circ}C}} = w\boldsymbol{K_{r,@25^{\circ}C}} + (1-w)\boldsymbol{K_{r,@100^{\circ}C}} \tag{5}$$

where the reduced SE stiffness at a given temperature is expressed as a linear interpolation of the stiffness matrices evaluated at neighboring temperatures. This approximation allows us to handle temperature dependent material properties where the temperature during thermal cycling is known and constant. This is certainly not the case for active thermal cycling (i.e., power cycling), where the actual temperature distribution is non-uniform and dependent on environmental conditions like convection coefficients. In this work, the authors begin with the hypothesis that approximate temperature distributions can be obtained by simulation (of the regular finite element model) using nominal conditions and material properties for components outside of the QFN. After this initial simulation, full field temperature distributions at different applied power levels during power cycling are obtained, see Fig 2.

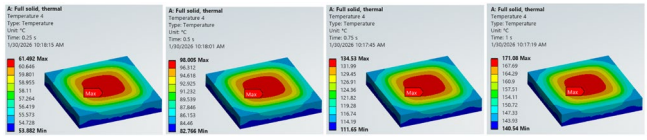


FIGURE 2: APPROXIMATE TEMPERATURE FIELDS AT DIFFERENT POWER VALUES

They can be used to evaluate the temperature-dependent material properties to obtain the SE stiffness matrix at individual temperature distributions corresponding to each power values. For the thermal SE stiffness during power cycling, it can again be expressed as a linear combination:

$$\boldsymbol{K_{r,@0.3W}} = w\boldsymbol{K_{r,@0.25W}} + (1-w)\boldsymbol{K_{r,@0.5W}} \tag{6}$$

where $\boldsymbol{K}_{r,@0.25W}$ denotes the SE stiffness matrix evaluated using the appropriate temperature field obtained at 0.25W. For power cycling simulations with a prescribed power cycle history, the weight factor w is a fixed and known function of time t. The same approximate temperature fields are used to generate the structural SE stiffness matrices at different powers for the thermal stress analysis.

B. Using SE in active thermal cycling simulations (Use pass)

After superelements (thermal and structural) at different applied power values are generated, they can be used in thermal cycling analyses. In a sequential thermal-stress analysis, the thermal analysis is carried out first. For a power cycling analysis where the power history is a known input, Eq (6) is implemented by adding all superelements at different power values to the same analysis, then scaling their stiffness matrix with the corresponding weight factors. This results in an equivalent SE whose stiffness changes piecewise linearly with the applied power. Once the temperature history is obtained from the thermal analysis, it can be mapped to the solder and PCB elements (modeled by regular solid elements) as known temperature distribution for thermal cycling. While for the structural SE (representing the QFN), it might be tempting to scale the individual SE matrices as a function power. However, it is important to remember that material properties are a function of temperature, not power. For thermal analysis, one can scale the matrices based on power since power is the direct input, while for structural analysis, the direct input is the mapped temperature field. As such, the weight factor w in structural analysis cannot simply be based on power and should instead be based on temperature. A simple scaling rule can be postulated based on the mean temperature of SE (obtained from nodal average of all master nodes):

$$w = \frac{T_{a,@0.5W} - T_{m,@0.3W}}{T_{a,@0.5W} - T_{a,@0.25W}} \quad (7)$$

where T_a denotes the (known) mean temperature of the QFN in the approximate temperature fields (see Table 1) and T_m denotes mean temperature of the SE master nodes obtained during the SE thermal analysis. $T_{m,@0.25W}$ and $T_{m,@0.5W}$ are known scalar quantities from the approximated temperature fields in Fig 1, $T_{m,@0.3W}$ is known after the SE thermal analysis is completed. Compared to the fixed weight factors (as a function of time) used in the thermal analysis, the weight factors in the structural analysis are not constant, it depends on the mean temperature of the SE obtained from the thermal analysis. This difference is significant, since different conditions (thermal conductivity and/or convection coefficients) might be used during the use pass that may lead to different temperature distributions in the model. A temperature-dependent weight factor captures this important variation with the limited information available in the SE solution.

TABLE 1: MEAN OF APPROXIMATED QFN TEMPERATURE FIELDS AT DIFFERENT POWER

Power [W]	0	0.25	0.5	0.75	1
T_a [℃]	25	57.3	89.6	121.9	154.24

With the weight factors for the structural SE determined, an equivalent nonlinear SE can be formed from the linear combination of the different SE matrices to account for material temperature-dependence in the structural analysis.

As with any piecewise linear approximation to nonlinear curves, the interpolation accuracy is expected to improve when more interpolation points are used. A convergence study is conducted to compare the SE solutions with different number of SE calculated at different power values with a reference solution conducted with regular solid finite elements (hence capturing full material temperature dependence). The results on the mean difference in plastic work density of the solders are shown in Table 2.

TABLE 2: COMPARISON OF SE SOLUTIONS USING DIFFERENT NUMBER OF POWER VALUES

Number of power values	Average error in solder plastic work density
1 (1W)	34.8%
2 (0,1W)	9%
3 (0,0.5,1W)	7.4%
5 (0,0.25,0.5,0.75,1W)	4.2%

A clear and monotonic reduction in error can be observed, indicating that the SE solution gradually approaches the full nonlinear temperature-dependent material behavior as the number of superelements (i.e., interpolation points) used in the analysis increases. With only 5 SE for both thermal and structural analysis, the mean error on the solder plastic work density falls to below 5%.

C. Sensitivity analysis

A core assumption in the current approach is that the approximate temperature fields at different power values (see Fig 2) are obtained with nominal material properties and conditions. This assumption is required since the actual material properties and thermal boundary conditions during use pass can vary and is not known a-priori when generating the superelements. The accuracy of the proposed workflow therefore hinges on the sensitivity of the SE solution with respect to the assumed material properties used when generating the approximate temperature fields. A sensitivity study is conducted in Ansys optiSLang [8] to elucidate its

effects. The following properties in the use pass are selected as input variables:

1. FR4 (PCB material) property scale factor (thermal and mechanical)
2. Copper property scale factor (thermal and mechanical)
3. Convection film coefficient

The following thermal and mechanical outputs are used to monitor the sensitivity with respect to input variations:

1. Error in SE temperature field compared to reference
2. Average error in solder plastic work
3. Maximum error in solder plastic work

50 design points were simulated in this work. Each input property is varied by ±25% compared to the nominal value. The relative importance matrix is shown in Table 3:

TABLE 3: RELATIVE IMPORTANCE OF INPUT VARIABLES TO DIFFERENT OUTPUTS

	FR4	Copper	Convection coefficient
Temperature error	6%	87%	7%
Avg error plastic work	44%	<1%	56%
Max error plastic work	46%	<1%	54%

For the thermal analysis, only the copper conductivity contributes significantly to the temperature prediction error between the SE and reference solution. This is reasonable because copper is also contained in the QFN, any variation in the material properties during the use pass will not be accounted for in the superelement representation of the QFN previously generated using nominal properties. While FR4 properties and convection coefficients are outside of the SE, so they also enter the use pass SE simulation as direct user inputs, the SE temperature solution will change naturally as the user inputs different FR4 and convection property values, hence the lower influence on temperature error. For the mechanical outputs, FR4 properties and convection coefficients play a significant role in errors in the solder plastic work since both properties significantly affect the resulting temperature distribution during use pass.

Choosing the top two most important input features for the temperature prediction error, the response surface contour is shown in Fig 3. For uniformity, the input property variations have been converted to percentages (relative to the assumed values used in the generation pass).

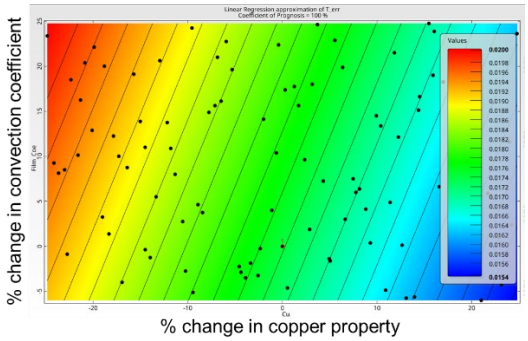


FIGURE 3: RESPONSE SURFACE CONTOUR OF SE TEMPERATURE PREDICTION ERROR

From the contour plot, it can be seen that the temperature prediction error for all input variations remains less than 0.05%, indicating that the effects of thermal properties temperature-dependence are negligible in this example, so the SE solution remains highly accurate despite the differences in input properties. The contour plots for the mean and max prediction error on the solder plastic work densities are shown in Figs 4 and 5.

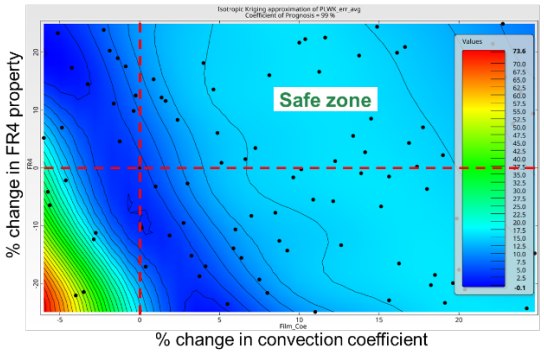


FIGURE 4: RESPONSE SURFACE CONTOUR OF MEAN ERROR IN SOLDER PLASTIC WORK DENSITY

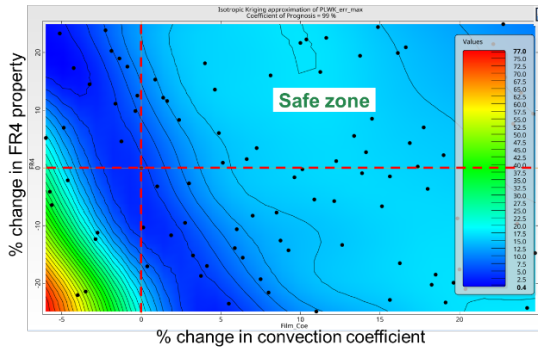


FIGURE 5: RESPONSE SURFACE CONTOUR OF MAX ERROR IN SOLDER PLASTIC WORK DENSITY

From the contour plot results, we can see that the mean and max error in plastic work density follow similar trends. The SE prediction error increases significantly when the FR4 properties and convection coefficient are reduced in the use

pass (lower left quadrant). While in all other quadrants, the prediction error between SE and the reference solution remains below 20% regardless of input property variations. This can be explained by the temperature based weighting scheme in Eq (7). When the FR4 conductivity and (more importantly) convection coefficient decreases, temperature in the use pass SE simulation will naturally increase. If the highest temperature seen during use pass exceeds that of the assumed temperature fields used during SE generation, then the temperature-based weighting scheme is no longer interpolating and instead extrapolating to unknown temperatures. This trend is directly visible when we plot the average plastic work prediction error with respect to difference in the max temperature in use pass and in the assumed temperature fields, see Fig 6.

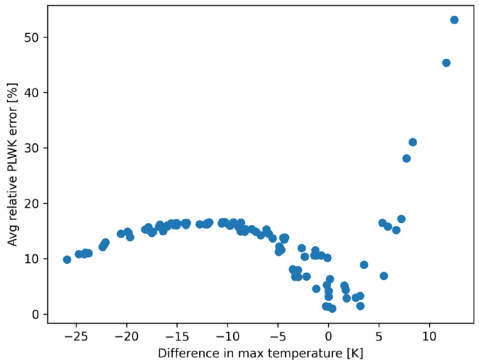


FIGURE 6: AVERAGE PLASTIC WORK DENSITY PREDICTION ERROR WRT DIFFERENCE IN MAX TEMPERATURE

Once the max temperature during use pass exceeds that seen in the generation pass (temperature difference > 0), the prediction error increases significantly. But within the interpolation range (temperature difference < 0), the prediction error remains less than 20%, which is quite stable considering that there are ±25% variations on the input properties.

III. Conclusion

This work investigates the creation and the use of superelement models that account for the temperature-dependent material properties and can be used in active thermal cycling simulations where the temperature distribution within the QFN and the PCB is nonuniform. The main idea is to obtain an approximate temperature distribution from nominal material properties and boundary conditions and use this temperature to evaluate SE at different applied power levels (hence with different temperatures). The equivalent, temperature-dependent SE can be constructed as a linear combination of SE evaluated at different power levels. The weight factors in the linear combination are power-dependent for the thermal SE analysis and temperature-dependent for the structural SE analysis. The resulting sequential thermal stress analysis using SE shows good agreement with the full solid element reference solution as the number of SE increases (i.e., increasing the number of interpolation points on the nonlinear temperature dependence curve), reaching error less than 5% when 5 SEs are used. Results of the sensitivity analysis show that the proposed approach is robust with respect to the assumed nominal properties used during the SE generation. The prediction error in solder plastic work remains less than 20% when the use pass material properties vary by ±25%. This proposed solution is a step towards overcoming the limitations of constant material properties in traditional SE workflows and shows great potential in capturing complex temperature dependence and the effect of nonlinear temperature distribution during active thermal cycling. These strengths make it a suitable tool for creating compact, IP-obfuscated models for capturing the QFN behavior in board-level electronics reliability analyses without having to share a detailed finite element model of the QFN.

References

[1] Pourhamid, R, Mahdavy Moghaddam, H and Mohammadzadeh, A. “Thermal analysis of functionally graded materials in cylinders and pistons based on super element method.” The Journal of Engine Research Vol. 30 No. 30 (2022): pp. 25–36.

[2] Jacques, Lionel, Bechet, Eric and Kerschen, Gaetan. “Finite element model reduction for space thermal analysis.” Finite Elements in Analysis and Design Vol. 127 (2017): pp. 6–15.

[3] Feuchter, Mike, Baumgartl, Hanna, Hanke, Martin, Rzepka, Sven and Wunderle, Bernhard. “Reduced-Order Model for Solder Balls–Potential of projection-based approaches for representing viscoplastic behavior.” 2024 25th International Conference on Thermal, Mechanical and Multi-Physics Simulation and Experiments in Microelectronics and Microsystems (EuroSimE): pp. 1–8. 2024. IEEE.

[4] Schleich, Florian, et al. "Superelement-based acceleration of finite-element simulations of wind turbine rotors." *Journal of Physics: Conference Series*. Vol. 2767. No. 5. IOP Publishing, 2024.

[5] “Ansys® Mechanical, Release 2026R1, Command Reference, ANSYS, Inc.” https://ansyshelp.ansys.com/account/secured?returnurl=/Views/Secured/corp/v261/en/ans_cmd/Hlp_C_CmdTOC.html

[6] Guyan, Robert J. “Reduction of stiffness and mass matrices.” AIAA journal Vol. 3 No. 2 (1965): pp. 380–380.

[7] Fischer, Sebastian, and Jürgen Wilde. "Modeling package-induced effects on molded Hall sensors." *IEEE transactions on advanced packaging* 31.3 (2008): 594-603.

[8] “Ansys® optiSLang, Release 2026R1, User Guide, ANSYS, Inc.” https://ansyshelp.ansys.com/account/secured?returnurl=/Views/Secured/corp/v2611/en/opti_ug/opti_ug.html